Please fill in the name of the event you are preparing this manuscript for.	SPE Annual Technical Conference and Exhibition	
Please fill in your 6-digit SPE manuscript number.	SPE-196136-MS	
Please fill in your manuscript title.	Experimental and Molecular Insights on Mitigation of Hydrocarbon Sieving in Niobrara Shale by CO ₂ Huff-n-Puff	

Please fill in your author name(s) and company affiliation.

Given Name	Surname	Company		
Ziming	Zhu	Colorado School of Mines		
Chao	Fang	Virginia Polytechnic Institute and State University		
Rui	Qiao	Virginia Polytechnic Institute and State University		
Xiaolong	Yin	Colorado School of Mines		
Erdal	Ozkan	Colorado School of Mines		

This template is provided to give authors a basic shell for preparing your manuscript for submittal to an SPE meeting or event. Styles have been included (Head1, Head2, Para, FigCaption, etc) to give you an idea of how your finalized paper will look before it is published by SPE. All manuscripts submitted to SPE will be extracted from this template and tagged into an XML format; SPE's standardized styles and fonts will be used when laying out the final manuscript. Links will be added to your manuscript for references, tables, and equations. Figures and tables should be placed directly after the first paragraph they are mentioned in. The technical content of your paper WILL NOT be changed. Please start your manuscript below.

Abstract

1 2

3

45

6

7

8

9

10

11 12

13

14

15

16 17

18 19

20

21

22

23

24

25

26

27

In nanoporous rocks, potential size/mobility exclusion and fluid-rock interactions in nano-sized pores and pore throats can turn the rock into a semi-permeable membrane, blocking or hindering the passage of certain molecules while allowing other molecules to pass freely. In this work, we conducted several experiments to investigate whether CO₂ can mitigate the sieving effect on the hydrocarbon molecules flowing through Niobrara samples. Molecular dynamics simulations of adsorption equilibrium with and without CO₂ were performed to help understand the trends observed in the experiments. The procedure of the experiments includes pumping of liquid binary hydrocarbon mixtures (C₁₀ C₁₇) of known compositions into Niobrara samples, collecting of the effluents from the samples, and analysis of the compositions of the effluents. A specialized experimental setup that uses an in-line filter as a mini-core holder was built for this investigation. Niobrara samples were cored and machined into 0.5-inch diameter and 0.7-inch length mini-cores. Hydrocarbon mixtures were injected into the mini-cores and effluents were collected periodically and analyzed using gas chromatography (GC). After observing the membrane behavior of the mini-cores, CO₂ huff-n-puff was performed at 600 psi, a pressure much lower than the miscibility pressure. CO₂ was injected from the production side to soak the sample for a period, then the flow of the mixture was resumed and effluents were analyzed using GC. Experimental results show that CO₂ huff-n-puff in several experiments noticeably mitigated the sieving of heavier component (C_{17}) . The observed increase in the fraction of C₁₇ in the produced fluid can be either temporary or lasting. In most experiments, temporary increases in flow rates were also observed. Molecular dynamics simulation results suggest that, for a calcite surface in equilibrium with a binary mixture of C₁₀ and C₁₇, more C₁₇ molecules adsorb on the carbonate surface than the C₁₀ molecules. Once CO₂ molecules are added to the system, CO₂ displaces C_{10} and C_{17} from calcite. The experimentally observed increase in the fraction of C_{17} thus can be attributed to the release of adsorbed C₁₇. This study suggests that surface effects play a significant role in affecting flows and compositions of fluids in tight formations. In unconventional oil reservoirs, observed enhanced recovery from CO₂ huff-n-puff could be partly attributed to surface effects in addition to the recognized gas-liquid interaction mechanisms.

3

4

5

6 7

8

9

10

11

12

13

14

15

16 17

18 19

20 21

22

23

2425

26

2728

29

30

31

32

33

34

35

36

37

38

39

40

41 42

43

44 45

46

47 48

49

Introduction

In today's North American field operations, CO₂ has become the most employed gas for EOR projects in tight reservoirs, due to its advantage in achieving miscibility with reservoir oils as well as the benefit of greenhouse gas sequestration. Among the various field injection schemes, huff-n-puff, a single-well cyclic process, is the most attractive for tight oil reservoirs. In CO₂ huff-n-puff, a producing well is first injected with CO₂. After a shut-in period (soaking), the well is put back on production. The efficacy of laboratory-scale cyclic CO₂ injection has been reported in a number of references: Tovar et al. (2014), Gamadi et al. (2014) and Ma et al. (2015) investigated the application potential of CO₂ huff-n-puff in nanoporous rocks through experiments. Song and Yang (2017) performed both experimental and simulation studies to evaluate the performance of CO₂ huff-n-puff process for the Bakken Formation, all pointing out that CO₂ huff-n-puff considerably improved the oil recovery.

Shale with clastic components is known to possess sieving properties to ionic species within an aqueous phase from electrostatic exclusion. In shale, because of the overlap of electrical double layers (EDL) that formed near the surface of naturally negatively charged clay platelets in contact with aqueous solution, certain anions approaching a pore throat coated with clay platelets may be retarded, leading to sieving of these anions across the shale. Wyllie (1948) measured the electrical potential across a shale placed between NaCl solutions with different concentrations and proved that shale can act as a semi-permeable membrane. Buneev et al. (1947) and Lomtadze (1954) experimentally investigated the salt-filtering properties of clays. Kemper (1960), McKelvey and Milne (1962), Kryukov et al. (1962), Englehardt and Gaida (1963) and Milne et al. (1964) reported that compacted clays can exclude salt ions, which again indicates the membrane properties of shale. Young and Low (1965) demonstrated experimentally that certain natural clayey rocks exclude salt ions and have membrane properties. Field-scale observations also indicate that shale can act as semi-permeable membranes. Berry (1959, 1960) found that the presence of chemical and pressure anomalies is widely distributed in the San Juan Basin of New Mexico and Colorado, which they believe can be best explained by chemical osmosis or salt filtration caused by membrane properties of shale. Bailey et al. (1961) also reported the existence of salt filtration in Wheeler Ridge anticline of the San Joaquin Valley, California. Recently, Neuzil (2000) showed that water transport between boreholes is interrelated with an applied chemical gradient through a nine-year in-situ field experiment which measures the fluid pressure and concentration on the Cretaceous Pierre Shale in South Dakota, confirming the significant role of membrane properties of shales.

In tight 'shale' formations, due to the abundance of micropores (< 2 nm) and mesopores (2-50 nm) (Kuila and Prasad 2013), it is reasonable to hypothesize that sieving could exist due to preferential adsorption or size/mobility exclusion, resulting in 'shale' reservoirs prone to producing lighter and more mobile components. Here, 'shale' refers to any tight, nanoporous rock that contains flowable hydrocarbons, and does not necessarily require richness in clay content. Currently, there is some evidence of membrane behavior of shale for hydrocarbons derived from observed compositional differences between hydrocarbons in the reservoir and its associated source rocks (Hunt and Jameson 1956, Brenneman and Smith 1958, Hunt 1961). Olsen (1969, 1972), Kharaka and Smalley (1976), and Whitworth (1993) pointed out that some level of sieving for hydrocarbon molecules in shale is attributed to size exclusion. Additionally, mineral surfaces can preferentially adsorb certain components over others (Cheng and Huang 2004; Heller and Zoback 2014; Wang et al. 2015), and such a mechanism could also generate membrane behavior when adsorbing surfaces are unsaturated. Kang et al. (2011) provided a mechanistic description of CO₂ uptake into shales, suggesting that the nanopores can behave as a molecular sieve in which CO₂ can reside but other molecules cannot due to preferential adsorption. Our previous publication, Zhu et al. (2019), firstly demonstrated the presence of sieving effect in Niobrara shale to hydrocarbon molecules (C₁₀ C₁₇). Through analysis of experimental data and mass balance calculations enabled by molecular dynamics simulations, Zhu et al. (2019) inferred that both size exclusion and preferential adsorption mechanisms should exist. This study is a continuation of Zhu et al.

 $\frac{24}{25}$

Experimental and Simulation Methodology

Prior to huff-n-puff tests, we performed filtration tests, which is a combination of a mini-core flooding test and a compositional analysis of the effluent using gas chromatography. The objective of filtration test is to check whether Niobrara shale possesses membrane properties to the selected hydrocarbon mixtures. In filtration tests, as schematically shown in figure 1, a liquid binary hydrocarbon mixture (C₁₀ C₁₇) was driven into a cylindrical rock sample inside a vertically placed core holder, The effluent fluid was collected using a collection vial sealed by deionized water to prevent evaporation, and then analyzed using gas chromatography (Agilent 7890B). The details of sample preparation, fluid collection, and experimental procedures can be found in our previous publication (Zhu et al. 2019).

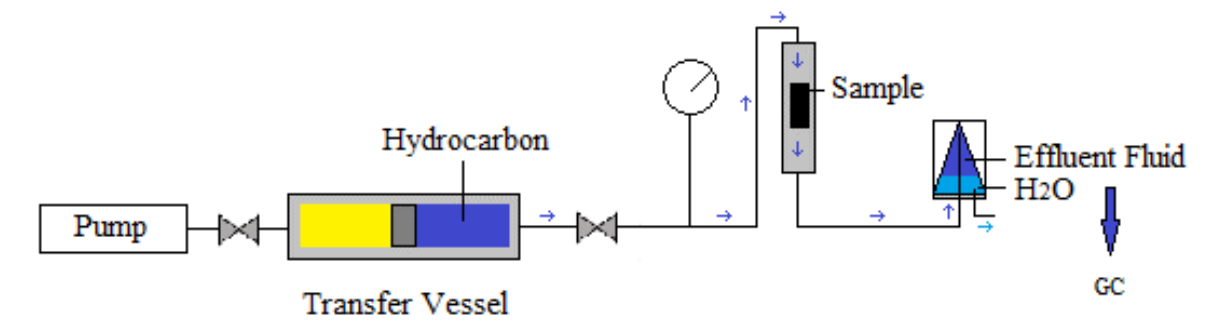


Figure 1. Schematic diagram of filtration test

Following the filtration tests, we performed one cycle of huff-n-puff using CO₂. First, we shut down hydrocarbon injection and disconnected the core holder from the pump and the transfer vessel. Then, as schematically shown in figure 2, after plugging the inlet of the core holder, we injected CO₂ from the producing side at 600 psi and soaked sample #1-3 for 10 days and sample #4-6 for 8 days. Note that at 600 psi CO₂ and our oil are immiscible. After soaking, we disconnected the core holder from the CO₂ tank, connected the core holder back to the pump and the transfer vessel, and resumed injection of oil around 2000 psi. We characterized the compositions of produced fluids after CO₂ soaking and compared the flow rates before and after CO₂ soaking. Note that compositions of all fluid samples were measured at the ambient condition and hence we did not detect any CO₂ in any of the liquid samples.

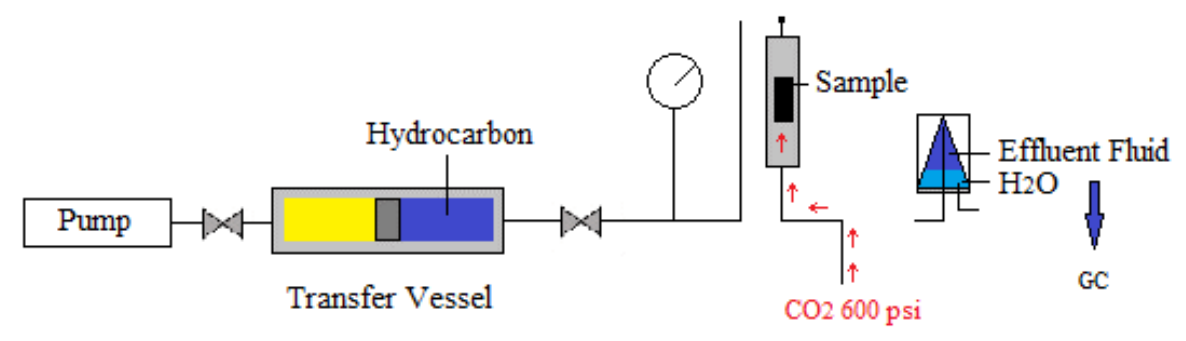


Figure 2. Schematic diagram of CO₂ huff-n-puff test

To investigate the mechanisms that have led to the compositional differences observed in the filtration tests and specifically preferential adsorption, we conducted molecular dynamics simulations of the mixture of C_{10} and C_{17} in equilibrium with a calcite surface approximating Niobrara shale in our prior study (Zhu et al. 2019). In this work, molecular dynamics (MD) simulation was also employed to study how CO_2 affects the equilibrium of C_{10} and C_{17} on the calcite surface.

Figure 3a shows the snapshots of our MD simulation systems. A \sim 8 nm thick mixture of linear alkanes of C_{10} , C_{17} and CO_2 were placed above a \sim 2 nm-thick model Niobrara substrate. The molar ratio between

 C_{10} and C_{17} was set to 4:1 to mimic the situation in the experiment. The hydrocarbon mixture and CO_2 were bounded by a piston that was fixed in space. The number of CO_2 molecules was adjusted by trial-and-error such that the gas pressure (the pressure on the piston) was 33 bar (479 psi), which is lower but comparable to the pressure applied in the experiment. The system is periodic in directions parallel to the calcite slab (x- and y-directions) while a vacuum space was placed outside of the piston to remove the periodicity in z-direction. To compare the adsorption without CO_2 , a reference system was set up as shown in figure 3b. A \sim 8 nm thick 4:1 mixture of C_{10} and C_{17} was used, the gas phase and piston were replaced with a large vacuum space in z-direction.

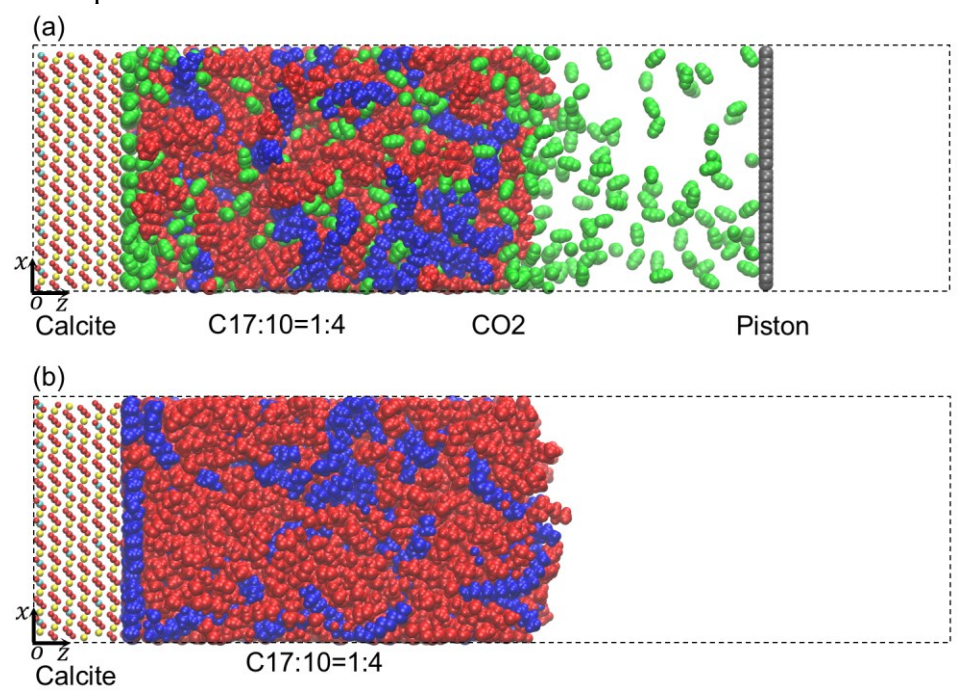


Figure 3. Snapshots of molecular dynamics simulation systems. (a) The system with a hydrocarbon mixture and CO₂ (C₁₀:C₁₇ = 4:1). (b) The system with only hydrocarbon mixture (C₁₀:C₁₇ = 4:1). The calcite is shown in small spheres (Calcium: yellow, Carbon: cyan, and Oxygen: red). The hydrocarbons and CO₂ are shown as van der Waals spheres (C₁₇ in blue, C₁₀ in red, and CO₂ in green). The piston atoms are shown in grey spheres. The simulation boxes are denoted using black dashed boxes.

Hydrocarbons were described using all atoms models. The OPLS-AA force fields for linear hydrocarbons with a recently optimized parameter set were applied for C₁₀ and C₁₇ (Siu et al. 2012). CO₂ was described using TraPPE force fields (Potoff and Siepmann 2001). Given that the major component of Niobrara shale is calcite (Kuila and Prasad 2013), the Niobrara substrate was again modeled as a calcite slab. The most stable and neutral plane of calcite was exposed to the hydrocarbons by cutting from the {1014} direction. The Lennard-Jones (LJ) potential and partial charges of calcite atoms were taken from the re-fitted Dove's potential (Rahaman et al. 2008). The calcite atoms were fixed in space during the simulation. The interatomic potentials between dissimilar atoms were obtained using geometric combination rule.

MD simulations were performed using the 5.1.4 version of Gromacs (Abraham et al. 2015). An NVT ensemble with velocity-rescale thermostat and a time constant of 2 ps at 300 K was adopted (Bussi et al. 2007). A global cutoff of 1.2 nm was used for computing the LJ potential and the particle mesh Ewald (PME) method was used to calculate the electrostatic interactions (Darden et al. 1993). The time step was 1 fs. The simulation for the system with CO₂ ran for 150 ns and data from the last 50 ns was used for analysis.

Experimental and Simulation Results

We performed filtration tests and subsequent CO₂ huff-n-puff tests on six Niobrara samples collected from a quarry in Longmont, Colorado. The quarry has excellent exposures of the Fort Hays limestone and up to the B Marl of the Smoky Hill chalk member of the Niobrara formation. Table 1 lists the parameters of

each Niobrara core sample used in the tests, including length, diameter, and pore volume. The pore volume of each sample was calculated based on an estimated porosity of 8% for Niobrara samples. Table 2 lists the duration of CO₂ soaking (huff) and production (puff) for each Niobrara sample.

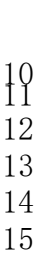
Table 1. Parameters of Niobrara core samples

Sample #	Length (in)	Diameter (in)	Pore Volume (cc)	
Niobrara Shale #1	0.735	0.5	0.189	
Niobrara Shale #2	0.704	0.5	0.181	
Niobrara Shale #3	0.741	0.5	0.191	
Niobrara Shale #4	0.688	0.5	0.177	
Niobrara Shale #5	0.716	0.5	0.184	
Niobrara Shale #6	0.731	0.5	0.188	

Table 2. Duration of CO₂ soaking in the 'huff' stage and production in the 'puff' stage of each sample in the huff-n-puff test

Sample #	CO ₂ Soaking, days	Production, days
Niobrara Shale #1	10	27
Niobrara Shale #2	10	14
Niobrara Shale #3	10	12
Niobrara Shale #4	8	11
Niobrara Shale #5	8	10
Niobrara Shale #6	8	11

Experimental results of Niobrara samples #1 – 6 are shown in figure 4 – 9. In each plot, x-axis is the amount of fluid in terms of pore volume produced from each sample, and y-axis is the fluid composition in terms of mole fraction of C_{10} . The red short line represents the mole fraction of C_{10} in the injected fluid that differed slightly for each sample. Blue short lines represent the mole fraction of C_{10} in the produced fluid before CO_2 injection. In each plot, the start of CO_2 injection and soaking (huff) is indicated by the vertical dashed line, with the left side being the period of filtration test and the right side being the period of production (puff) stage. The orange and green short lines through which the dashed line passes represent the mole fraction of C_{10} in the fluid upstream of the core holder or in the remaining injection fluid before and after CO_2 soaking, respectively. Each data point (marked by -) is the average of two consecutive GC measurements marked by up (\land) and down (\lor) arrows, which respectively represent the 1st and the 2nd GC measurements. For the benefit of a comprehensive evaluation, we summarized the initial composition of the injected fluid, range of C_{10} mole fraction recorded in the produced fluid, and C_{10} mole fraction in the upstream fluid for each Niobrara sample before and after CO_2 soaking in table 3.



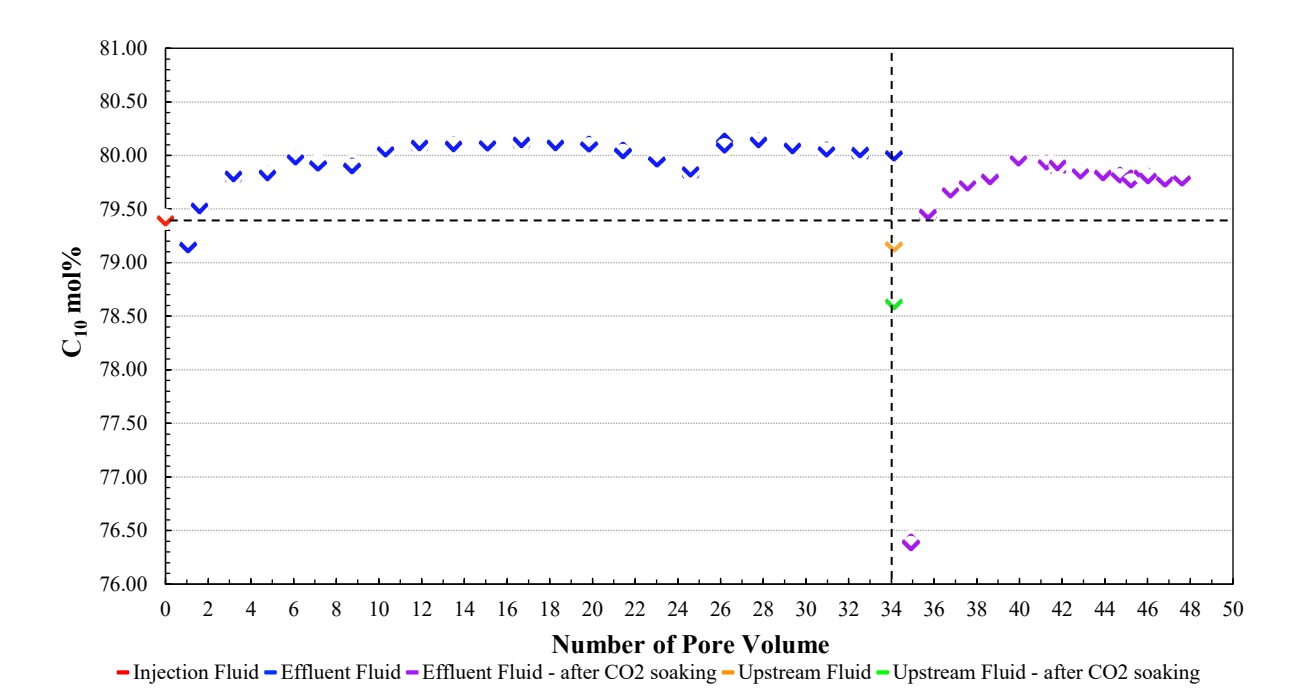


Figure 4. Experimental result of Niobrara shale sample #1

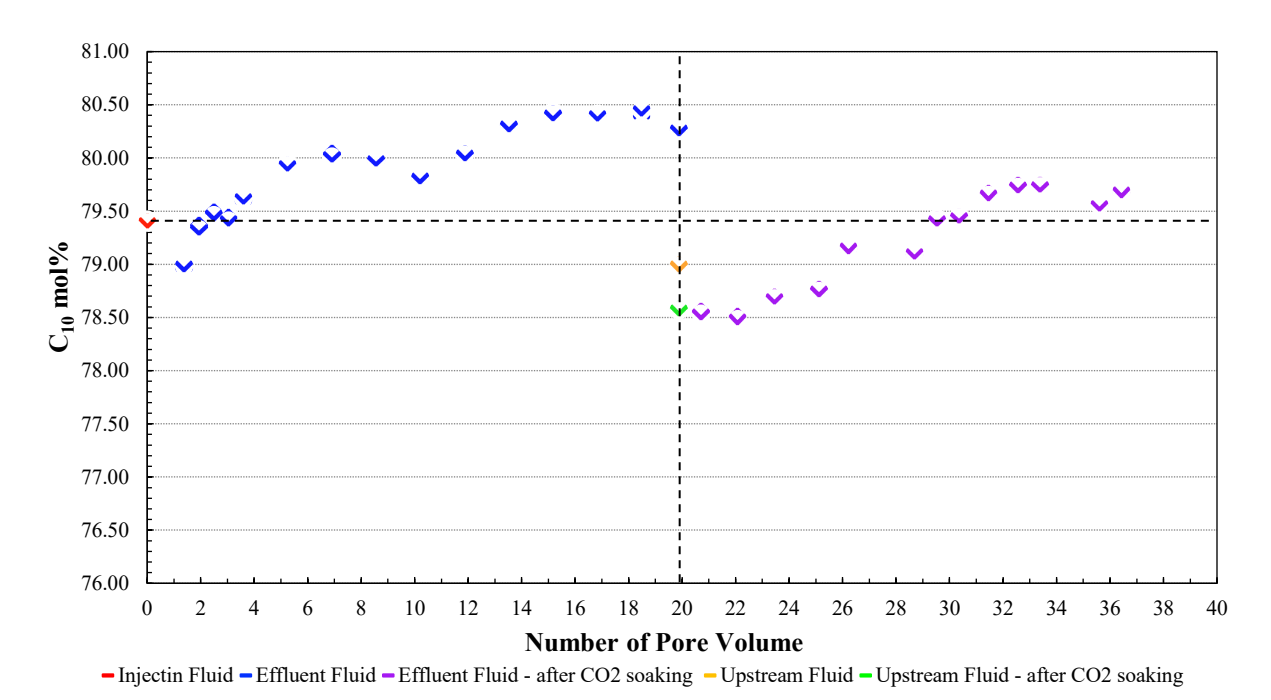
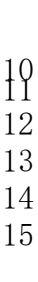
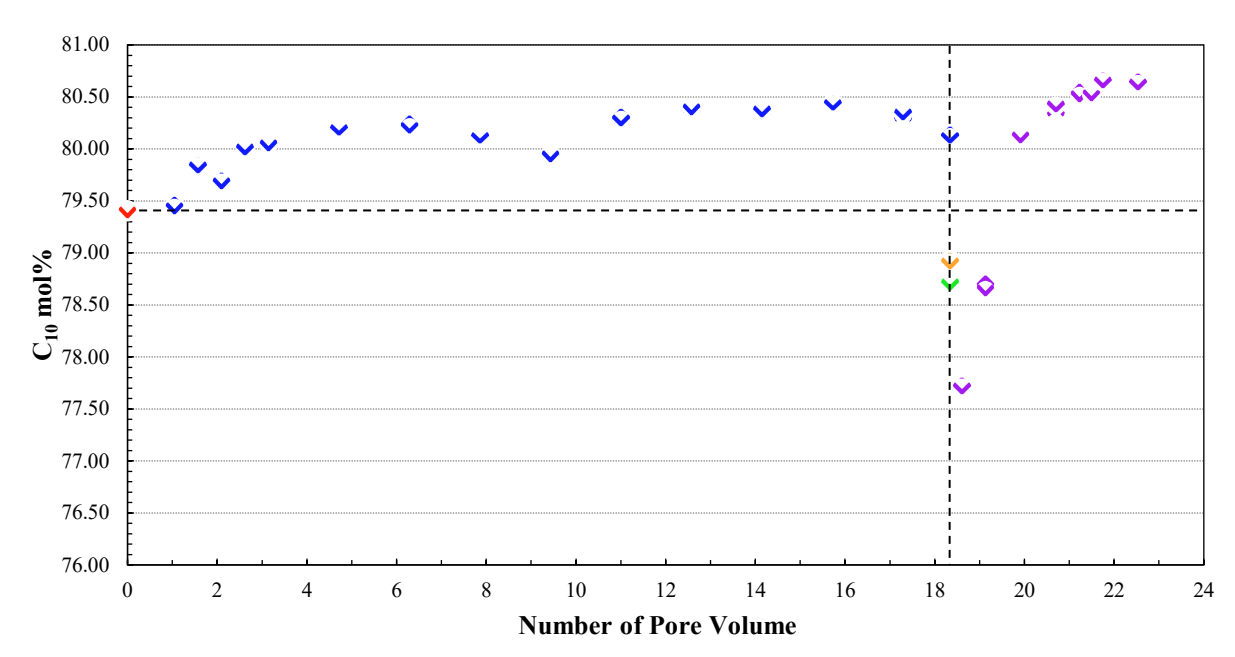


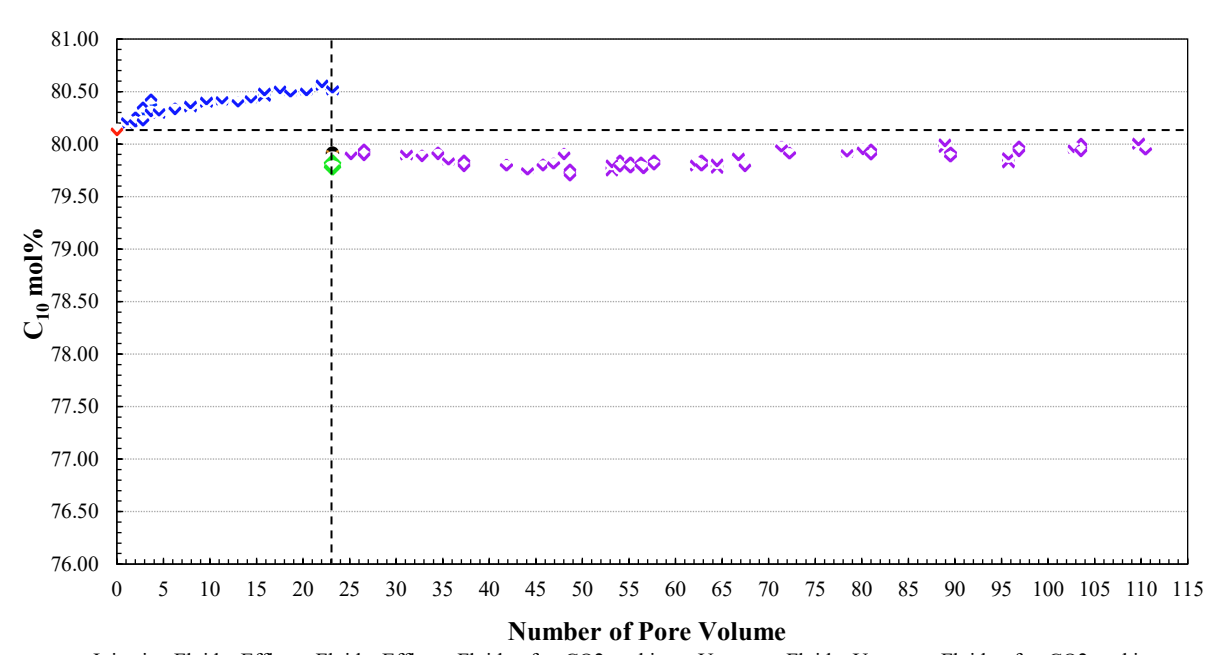
Figure 5. Experimental result of Niobrara shale sample #2





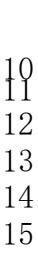
- Injection Fluid - Effluent Fluid - Effluent Fluid - after CO2 soaking - Upstream Fluid - Upstream Fluid - after CO2 soaking

Figure 6. Experimental result of Niobrara shale sample #3



- Injection Fluid - Effluent Fluid - Effluent Fluid - after CO2 soaking - Upstream Fluid - Upstream Fluid - after CO2 soaking

Figure 7. Experimental result of Niobrara shale sample #4



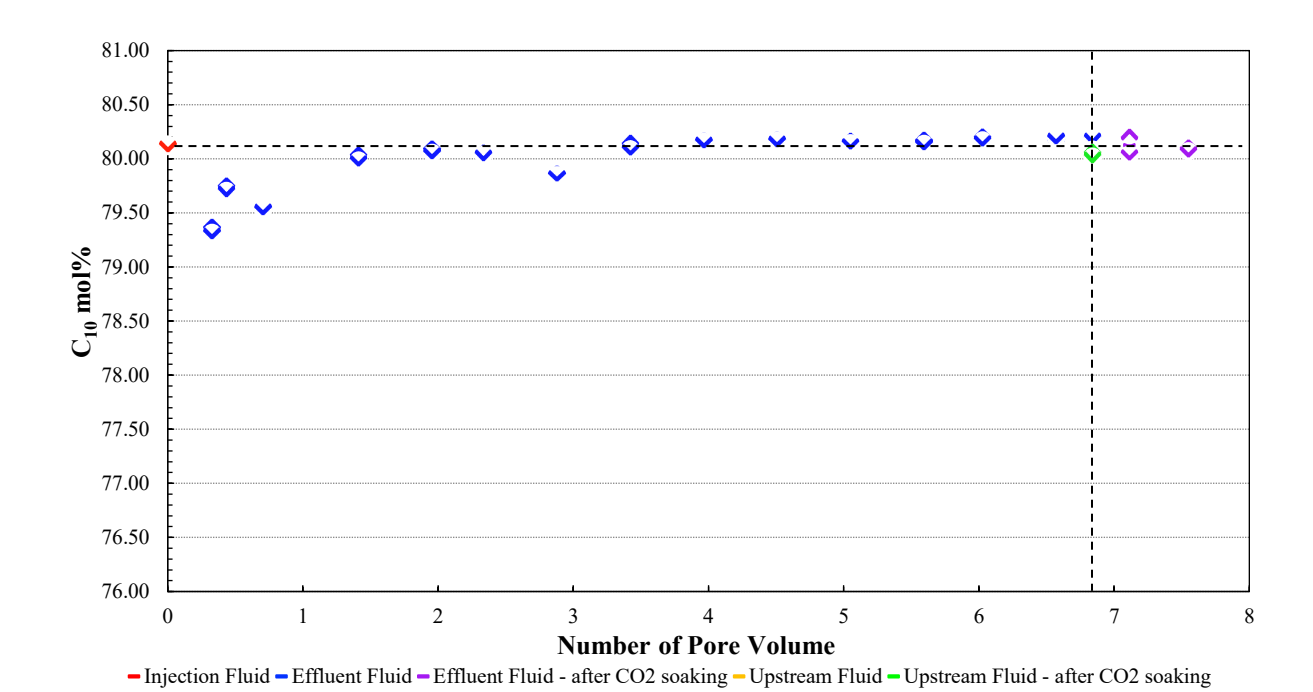


Figure 8. Experimental result of Niobrara shale sample #5

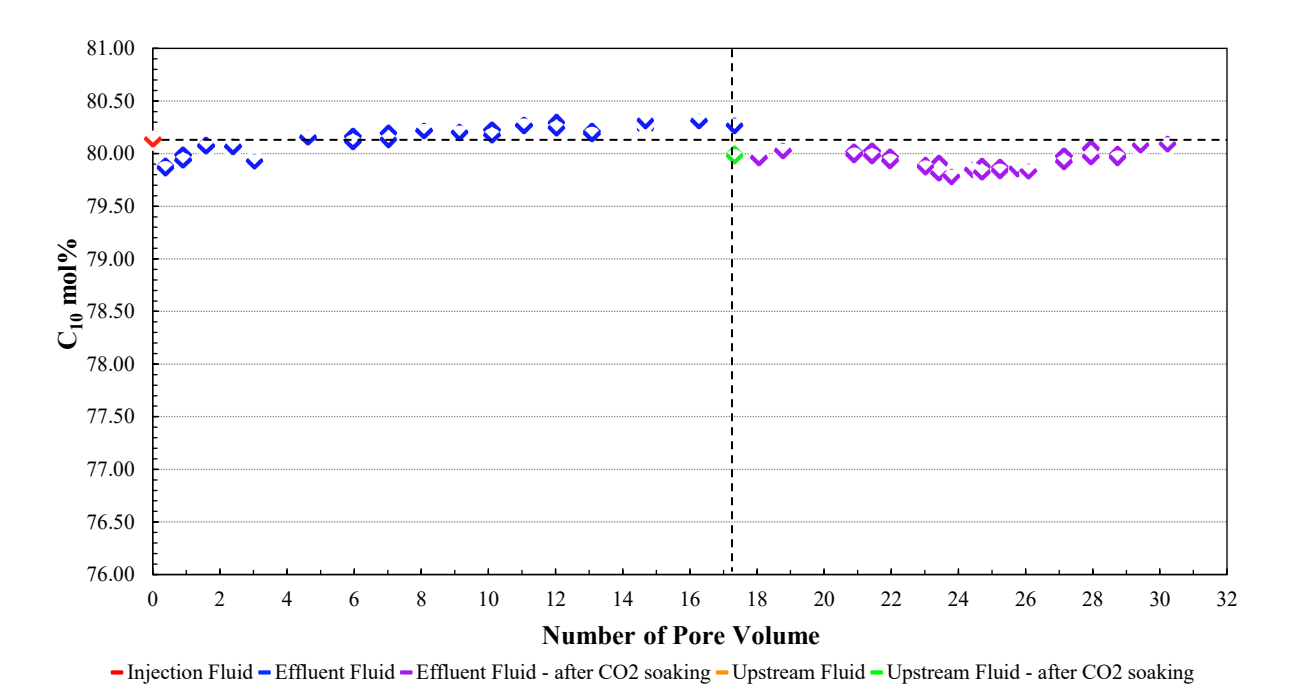


Figure 9. Experimental result of Niobrara shale sample #6

Table 3. Summar	v of fluids com	positions (C ₁	10 mol%) before	and after CO ₂ s	oaking

Sample #	Injected Fluid	Produced Fluid		Upstream Fluid	
Sample #	C ₁₀ mol%	Before Soaking	After Soaking	Before Soaking	After Soaking
Niobrara Shale #1	79.41	79.16 - 80.14	76.39 - 79.96	79.17	78.62
Niobrara Shale #2	79.41	78.98 - 80.43	78.51 - 79.75	79.00	78.58
Niobrara Shale #3	79.41	79.46 - 80.44	77.72 - 80.66	78.92	78.71
Niobrara Shale #4	80.12	80.20 - 80.56	79.73 – 80.00	79.92	79.80
Niobrara Shale #5	80.12	79.35 - 80.20	80.10 – 80.13	80.05	80.05
Niobrara Shale #6	80.12	79.87 - 80.31	79.78 – 80.09	80.03	79.99

We note that the compositional data prior to CO_2 soaking were already presented in our previous paper (Zhu et al. 2019). These compositional data indicate that the heavier component (C_{17}) in the injected fluid was noticeably hindered and the mole fraction of lighter component (C_{10}) in the produced fluid had various degrees of increase compared with the injected fluid, of which Niobrara sample #1 – 4 changed relatively more significantly, and Niobrara sample #5 and #6 changed relatively mildly. Oppositely, C_{10} mole fraction in the fluid upstream of each Niobrara sample decreased, indicating that the remaining injection fluid became heavier. These observations all point to the existence of sieving in our Niobrara samples.

After CO₂ soaking, for all Niobrara samples except sample #5, C_{10} mole fraction in the upstream fluid further decreased slightly, suggesting that CO_2 that reached the fluid upstream of the samples may have preferentially vaporized some C_{10} . After continuation of injection, C_{10} mole fractions in the first or the first few pore volumes of produced fluid were consistently less than the C_{10} mole fraction in the original fluid (red point), suggesting that CO_2 mitigated sieving and allowed the heavier component (C_{17}) that was filtered to flow through. For sample #5, based on the observations made from the experiment, during soaking, sample #5 did not show any signs of CO_2 breakthrough into the upstream fluid, indicating that sample #5 did not permit CO_2 penetration, and hence presented itself as an anomaly. After production of a few pore volumes, C_{10} mole fraction in the produced fluid of sample #1, #2 and #3 gradually increased to become higher than the C_{10} mole fraction in the original fluid, indicating that the heavier component (C_{17}) was hindered again, consistent with the situation before CO_2 huff-n-puff. Conversely, for sample #4 and #6, as production continued, C_{10} mole fraction in the produced fluid was always lower than that of the original fluid, without recurrence of sieving of C_{17} .

In addition to compositional changes, we observed increases in the rates of production after CO₂ soaking. The average flow rates, expressed in terms of pore volumes produced per day, of Niobrara samples before and after CO₂ soaking are calculated as

$$\bar{q} = \frac{N_{PV_produced}}{T_{production}} \dots (1)$$

 and summarized in table 4. N_{PV_produced} is the number of pore volumes of fluid produced from each sample before or after CO₂ soaking, and T_{production} is the corresponding production time expressed in days. It can be noticed from the results that, except sample #5, of which no CO₂ penetration was observed, the average flow rates of all Niobrara samples increased at various degrees, with the highest about 10 fold.

 However, it was also observed from most samples that the production rates after CO₂ soaking gradually decreased over time, approaching the level before CO₂ soaking.

Table 4. Production rates before and after CO₂ soaking

Comple #	Average Flow Rate (PV/day)			
Sample # —	Before CO ₂ Soaking	After CO ₂ Soaking	After/Before	
Niobrara Shale #1	0.42	0.50	1.19	
Niobrara Shale #2	0.28	1.18	4.21	
Niobrara Shale #3	0.25	0.35	1.40	
Niobrara Shale #4	0.70	7.94	11.34	
Niobrara Shale #5	0.21	0.08	0.38	
Niobrara Shale #6	0.53	1.17	2.21	

The preferential adsorption of C_{17} over C_{10} near calcite surface in absence of CO_2 from MD simulations is shown in figure 10a (from the carbon atoms) and figure 10b (from the center of mass of C_{10} and C_{17}). The hydrocarbon mixture shows distinct layers near the calcite surface and the first layer of hydrocarbon is dominated by C_{17} molecules. The adsorption of C_{10} and C_{17} on the calcite surface is quantified by defining a surface excess as

$$\Gamma_{S} = \int_{0}^{z_{2}} \rho(z)dz - (z_{2} - z_{1})\rho_{bulk} \dots (2)$$

where $\rho(z)$ is the number density of hydrocarbon as a function of z. ρ_{bulk} is the corresponding number density of the hydrocarbon in the bulk mixture, z_1 is the nominal lower boundary of the hydrocarbon mixture and z_2 is the position at which the hydrocarbon density approaches bulk value (marked using dashed lines in figure 10).

Considering the effective space occupied by hydrocarbons molecules (figure 10a and 10b), we set z_1 to be the position of the first peak of carbon atoms and z_2 to be 8 nm. The surface excesses were measured to be $\Gamma_s^{C_{10}} = 5.56 \times 10^{-2} \text{ nm}^{-2}$ and $\Gamma_s^{C_{17}} = 1.80 \times 10^{-1} \text{ nm}^{-2}$ based on the center of mass of hydrocarbon molecules. These results show that both C_{10} and C_{17} were enriched near calcite surface and strong preferential adsorption exists for C_{17} molecules. Specifically, $\Gamma_s^{C_{17}}/\Gamma_s^{C_{10}} = 3.24$ is more than 10 times of $\rho_{\text{bulk}}^{C_{17}}/\rho_{\text{bulk}}^{C_{10}} = 0.25$ in bulk mixture.

The density profiles after introducing CO₂ are shown in figure 10c (from carbon atoms of hydrocarbon and the center of mass of CO₂) and figure 10d (from the center of mass of all molecules). Near calcite surface, the adsorption of hydrocarbon was modified greatly by CO₂. First, as shown in figure 10c and 10d, CO₂ was adsorbed on calcite with a prominent peak as high as 80 nm⁻³. Second, C₁₀ and C₁₇ were displaced from the calcite surface. They were, instead, in contact with the CO₂ layer and developed a structured interface, as indicated by the oscillations in the density profiles slightly beyond z = 2 nm in figure 10c and 10d. Using the surface excess defined above, the surface excesses based on the center of mass of hydrocarbon molecules at this interface were found to be $\Gamma_s^{C_{10}} = 3.75 \times 10^{-1}$ nm⁻² and $\Gamma_s^{C_{17}} = 9.83 \times 10^{-3}$ nm⁻² ($\Gamma_s^{C_{10}}/\Gamma_s^{C_{17}} = 38.10$ is about 10 times of $\rho_{\text{bulk}}^{C_{10}}/\rho_{\text{bulk}}^{C_{17}} = 4$ in bulk mixture). These values

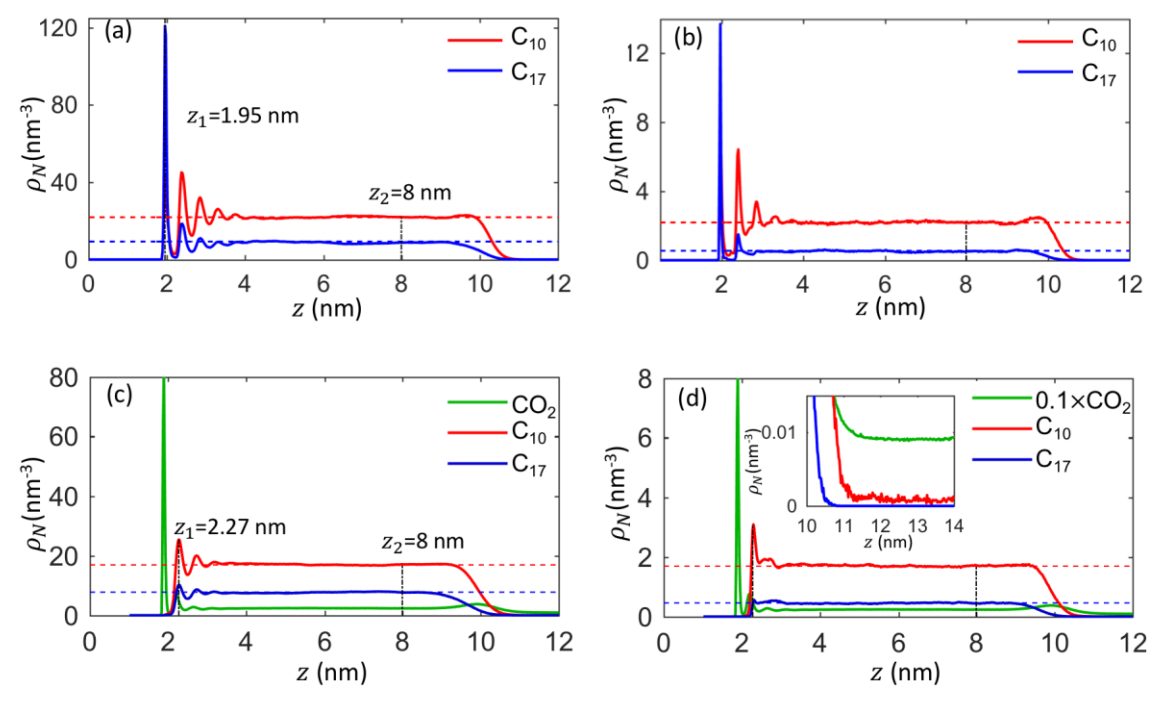


Figure 10. Density profiles of hydrocarbon mixtures near calcite surface. (a, c) The density profiles based on the carbon atoms of hydrocarbon for system without CO_2 (a) and with CO_2 (b), d) The density profiles based on the center of mass of hydrocarbons for system without CO_2 (b) and with CO_2 (d). z_1 is the position of first adsorption peak of carbon atoms. z_2 is the position where the density reaches bulk value. The inset in (d) shows the density profiles in the gas phase based on the center of mass of molecules. The density of CO_2 is scaled by 0.01.

These (rather) significant changes in the structure of fluids with introduction of CO₂, we think, are the results of two molecular-scale features of the system. First, CO₂ molecules have stronger electrostatic interactions with a calcite surface than C₁₀ and C₁₇, and this leads to the observed enrichment of CO₂ over these hydrocarbon molecules. Second, the adsorption of hydrocarbons is not only controlled by the electrostatic interactions but also the entropic penalty of long-chain hydrocarbons that must conform with the flat calcite surface. In the absence of CO₂, C₁₇ molecules reached calcite surface closely and their strong interactions with calcite overwhelmed the entropy penalty. We specifically observed that many C₁₇ molecules adopted a co-planar configuration on the surface. Because there are more atoms in a C₁₇ molecule than in C₁₀, the C₁₇-calcite interaction energy is lower and thus C₁₇ was preferentially enriched near the calcite surface. In the presence of CO₂, both C₁₇ and C₁₀ were displaced from the surface and their interactions with calcite were weakened. The entropic penalty of packing long-chain hydrocarbons near a planar surface might have become more important. Because the entropic penalty of packing C₁₇ with a longer chain is higher than that for C₁₀, the interface between the CO₂ layer and the bulk mixture became enriched with C₁₀.

Discussions

The results of molecular dynamics simulation show that CO_2 can displace most C_{17} molecules and C_{10} molecules adsorbed on the calcite surface, and this displacement eliminated the preferential adsorption of C_{17} over C_{10} . As C_{17} molecules are eluted from the surface of calcite minerals, it is reasonable that more C_{17} molecules were noticed in the produced fluid after CO_2 soaking. In the filtration tests prior to huff-n-

puff tests, C_{17} accumulated inside the Niobrara samples. Hence, it is not surprising that C_{17} mole fraction in the produced fluid after CO_2 soaking became higher relative to that of the original fluid. Considering that we observed increases of C_{17} mole fraction in five of the six Niobrara samples, this observed mitigation is likely a robust effect from CO_2 huff-n-puff.

Molecular dynamics simulation results show that a non-negligible amount of C_{10} molecules were vaporized into the gas phase (CO₂), whereas the vaporization of C_{17} was negligible. Therefore, in principle, other than elution, vaporization of C_{10} into the gas phase can also lead to an increase of C_{17} mole fraction in the produced fluid. However, as the molar amount of gas produced from each Niobrara sample was much less than that of liquid, the influence of this mechanism should be very limited in our experiments.

The observed increase in flow rate may be due to the reduction in viscosity of the bulk mixture due to CO₂ dissolution. Molecular dynamics simulation results show that the molar fraction of CO₂ in the liquid phase of the bulk mixture is around 50 mol% under soaking condition, which may potentially lead to a viscosity reduction of the liquid phase under production condition from about 1.35 cp before soaking to 0.44 cp after soaking. The viscosities were estimated through a multi-step process that involved separate correlations (Beggs and Robinson 1975; Vazquez and Beggs 1980; Egbogah and Ng 1990; Fitzgerald 1994) for each step of the process.

The Niobrara samples tested in the experiment were collected from an outcrop in Colorado. Its mineral composition (Tectosilicates, 11.3% by volume; Carbonates, 76.4% by volume; Clay, 10.7% by volume; Other, 1.6% by volume) is dominated by calcite and does not contain kerogen. For this reason, our molecular dynamics simulation focused on the interactions between C₁₀, C₁₇ molecules and calcite slabs. Flow of realistic hydrocarbon mixtures through tight formations may be controlled by many more parameters, e.g., the existence of kerogen and other minerals, solution-sorption equilibriums of various hydrocarbon species on surfaces can all influence sieving. Several studies noted that kerogen, though small in volume, can have an important effect in terms of adsorbing heavy components (Herdes et al. 2018; Liu and Chapman 2019). Morphology and flexibility of kerogen have been shown to affect sorption and transport (Tesson and Firoozabadi 2018). In a more integrated and more realistic model, the above effects of mineralogy and complexity of fluids on sorption and transport with and without the presence of CO₂ should all be considered.

Conclusions

In our previous study (Zhu et al. 2019), we confirmed that Niobrara shale has the ability to sieve hydrocarbons, allowing the passage of lighter components and hindering the transport of heavier components. In this study, we explored the effect of CO₂ huff-n-puff on the sieving ability of six Niobrara samples. We observed that the hindrance of heavier component (C₁₇) was clearly mitigated in five of the six samples. Additionally, the production rates of these five samples were stimulated to various degrees after soaking with CO₂. After resuming production for a certain period, recurrence of sieving was observed in three Niobrara samples, the production rates also gradually decreased to the levels before soaking.

Molecular dynamics simulation results suggest that mitigation of sieving was likely caused by elution of adsorbed C₁₇ by the injected CO₂. Adsorbed C₁₇ is prone to be replaced by CO₂ molecules. Increase in the flow rate could be resulted from CO₂ dissolution. However, more detailed analysis is definitely needed to understand sample-to-sample variations. This experimental study is the first evidence that CO₂ can mitigate the sieving of hydrocarbons in nanoporous reservoir rocks. Molecular dynamics simulations indicate that this benefit is likely associated with surface phenomena of CO₂. Surface mechanisms have not been considered in modeling of CO₂-EOR in unconventional tight oil reservoirs and they should be worthy topics for future investigations.

3

4

Acknowledgment

The authors at Colorado School of Mines would like to thank the Unconventional Reservoir Engineering Project (UREP) consortium at Colorado School of Mines for financial supporting this research project.

R.Q. and C. F. gratefully acknowledge the support of NSF under grant number CBET 1705287.

5 6 7

49

References

- 8 Abraham, M. J., Murtola, T., Schulz, R. et al. 2015. GROMACS: High Performance Molecular Simulations through Multi-9 Level Parallelism from Laptops to Supercomputers. SoftwareX 1-2: 19-25. https://doi.org/10.1016/j.softx.2015.06.001.
- 10 Bailey, E. H., Snavely, P. D. Jr., and White, D. E. 1961. Chemical Analysis of Brines and Crude Oil, Cymric Field, Kern 11 County, California. In Short Papers in the Geologic and Hydrologic Sciences, Articles 293-435: Geological Survey Research

12 1961, 306-309. Washington, D.C.: United States Government Printing Office.

- 13 Beggs, H. D. and Robinson, J. R. 1975. Estimating the Viscosity of Crude Oil Systems. Journal of Petroleum Technology 14 27(9): 1140-1141. https://doi.org/10.2118/5434-PA.
- 15 Berry, F. A. F. 1959. Hydrodynamics and Geochemistry of the Jurassic and Cretaceous Systems in the San Juan Basin, 16 Northwestern New Mexico and South-western Colorado. Ph.D. Thesis, Stanford University, Stanford, California (January 17 1959).
- 18 Berry, F. A. F. 1960. Geologic Field Evidence Suggesting Membrane Properties of Shales. American Association of Petroleum 19 Geologists Bulletin 44(6): 953-954.
- 20 Brenneman, M. C. and Smith, P. V. 1958. The Chemical Relationships Between Crude Oils and Their Source Rocks. In Habitat 21 of Oil: A Symposium, ed. L. G. Weeks, 818-849. Tulsa, Oklahoma: American Association of Petroleum Geologists.
- 22 Buneev, A. N., Kryukov, P. A., and Rengarten, E. V. 1947. Experiment in Squeezing Out of Solutions from Sedimentary 23 Rocks. Doklady Akademii Nauk SSSR 57(7): 707-709.
- 24 Bussi, G., Donadio, D., and Parrinello, M. 2007. Canonical Sampling through Velocity Rescaling. Journal of Chemical Physics 25 126(1):014101. https://doi.org/10.1063/1.2408420.
- 26 Cheng, A. L. and Huang, W. L. 2004. Selective Adsorption of Hydrocarbon Gases on Clays and Organic Matter. Organic 27 Geochemistry 35(4): 413-423. https://doi.org/10.1016/j.orggeochem.2004.01.007.
- 28 Darden, T., York, D., and Pedersen, L. 1993. Particle Mesh Ewald: An N·Log (N) Method for Ewald Sums in Large Systems. 29 Journal of Chemical Physics 98(12): 10089-10092. https://doi.org/10.1063/1.464397.
- 30 Englehardt, W. V. and Gaida, K. H. 1963. Concentration Changes of Pore Solutions During the Compaction of Clay Sediments. 31 Journal of Sedimentary Research 33(4): 919-930. https://doi.org/10.2110/33.4.919.
- 32 Fitzgerald, D. J. 1994. A Predictive method for Estimating the Viscosity of Undefined Hydrocarbon Liquid Mixtures. M.S. 33 Thesis, Pennsylvania State University, State College, Pennsylvania.
- 34 Gamadi, T. D., Sheng, J. J., Soliman, M. Y. et al. 2014. An Experimental Study of Cyclic CO₂ Injection to Improve Shale Oil 35 Recovery. Presented at the SPE Improved Oil Recovery Symposium, Tulsa, Oklahoma, 12-16 April. SPE-169142-MS. 36 http://doi.org/10.2118/169142-MS.
- 37 Heller, R. and Zoback, M. 2014. Adsorption of methane and Carbon Dioxide on Gas Shale and Pure Mineral Samples. *Journal* 38 of Unconventional Oil and Gas Resources 8: 14-24. https://doi.org/10.1016/j.juogr.2014.06.001.
- 39 Herdes, C., Petit, C., Mejía, A. et al. 2018. Combines Experimental, Theoretical, and Molecular Simulation Approach for the 40 Description of the Fluid-Phase Behavior of Hydrocarbon Mixtures within Shale Rocks. Energy Fuels 32(5): 5750-5762.
- 41 https://doi.org/10.1021/acs.energyfuels.8b00200.
- 42 Hunt, J. M. 1961. Distribution of Hydrocarbons in Sedimentary Rocks. Geochimica et Cosmochimica Acta 22(1): 37-49. 43 https://doi.org/10.1016/0016-7037(61)90071-0.
- 44 Hunt, J. M. and Jameson, G. W. 1956. Oil and Organic Matter in Source Rocks of Petroleum. American Association of 45 Petroleum Geologists Bulletin 40(3): 477-488.
- 46 Kang, S. M., Fathi, E., Ambrose, R. J. et al. 2011. Carbon Dioxide Storage Capacity of Organic-Rich Shales. SPE Journal 47 16(4): 842-855. https://doi.org/10.2118/134583-PA.
- 48 Kemper, W. D. 1960. Water and Ion Movement in Thin Films as Influenced by the Electrostatic Layer of Cations Associated Science
- 50 https://dx.doi.org/10.2136/sssaj1960.03615995002400010013x.

Mineral

51 Kharaka, Y. K. and Smalley, W. C. 1976. Flow of Water and Solutes Through Compacted Clays. American Association of 52

Society

of

America

journal

24(1):

10-16.

Petroleum Geologists Bulletin 60(6): 973-980. 53

Surfaces.

- Kryukov, P. A., Zhuchkova, A. A., and Rengarten, E. V. 1962. Changes in the Composition of Solutions Pressed from Clays
- 54 and Ion Exchange Resins. Doklady Akademii Nauk SSSR Earth Sci. Sect. 144(6): 167-169.

Soil

- 55 Kuila, U. and Prasad, M. 2013. Specific Surface Area and Pore-Size Distribution in Clays and Shales. Geophysical Prospecting
- 56 61(2): 341-362. https://dx.doi.org/10.1111/1365-2478.12028.

- Liu, J. and Chapman, W. G. 2019. Thermodynamic Modeling of the Equilibrium Partitioning of Hydrocarbons in Nanoporous 2 Kerogen Particles. Energy Fuels 33(2): 891-904. https://doi.org/10.1021/acs.energyfuels.8b03771.
- 3 Lomtadze, V. D. 1954. About the Role of Compaction Processes of Clayey Deposits in the Formation of Underground Waters.
- 4 Doklady Akademii Nauk SSSR 98(3): 451-454.
- 5 Ma, J., Wang, X., Gao, R. et al. 2015. Enhanced Light Oil Recovery from Tight Formations through CO₂ Huff'n' Puff Processes.
- 6 7 Fuel 154(15): 35-44. https://doi.org/10.1016/j.fuel.2015.03.029.
- McKelvey, J. G. and Milne, I. H. 1962. The Flow of Salt Solutions Through Compacted Clay. Proc., Ninth National Conference
- 8 on Clays and Clay Minerals, Purdue University, Lafayette, Indiana, 5-8 October, 248-259. https://doi.org/10.1016/B978-1-9 4831-9842-2.50017-1.
- 10 Milne, I. H., McKelvey, J. G., and Trump, R. P. 1964. Semi-permeability of Bentonite Membranes to Brines. American 11 Association of Petroleum Geologists Bulletin 48(1): 103-105.
- 12 Neuzil, C. E. 2000. Osmotic Generation of 'Anomalous' Fluid Pressures in Geological Environments. Nature 403: 182-184.
- 13 https://dx.doi.org/10.1038/35003174.
- 14 Egbogah, E. O. and Ng, J. T. 1990. An Improved Temperature-Viscosity Correlation for Crude Oil Systems. Journal of
- 15 Petroleum Science and Engineering 4(3): 197-200. https://doi.org/10.1016/0920-4105(90)90009-R.
- 16 Olsen, H. W. 1969. Simultaneous Fluxes of Liquid and Charge in Saturated Kaolinite. Soil Science Society of America journal
- 17 33(3): 338-344. https://dx.doi.org/10.2136/sssaj1969.03615995003300030006x.
- 18 Olsen, H. W. 1972. Liquid Movement Through Kaolinite Under Hydraulic, Electric and Osmotic Gradients. American
- 19 Association of Petroleum Geologists Bulletin **56**(10): 2022-2028.
- 20 Potoff, J. J. and Siepmann, J. I. 2001. Vapor-Liquid Equilibria of Mixtures Containing Alkanes, Carbon Dioxide, and Nitrogen.
- 21 AIChE Journal 47(7): 1676-1682. https://doi.org/10.1002/aic.690470719.
- 22 Rahaman, A., Grassian, V. H., and Margulis, C. J. 2008. Dynamics of Water Adsorption onto a Calcite Surface as a Function
- 23 of Relative Humidity. Journal of Physical Chemistry 112(6): 2109-2115. https://dx.doi.org/10.1021/jp077594d.
- 24 Siu, S. W., Pluhackova, K., and Böckmann, R. A. 2012. Optimization of the Opls-As Force Field for Long Hydrocarbons.
- 25 Journal of Chemical theory and Computation 8(4): 1459-1470. https://dx.doi.org/10.1021/ct200908r.
- 26 Song, C. Y. and Yang, D. Y. 2017. Experimental and Numerical Evaluation of CO₂ Huff-n-Puff Processes in Bakken
- 27 Formation. Fuel 190(15): 145-162. https://doi.org/10.1016/j.fuel.2016.11.041.
- 28 Tesson, S. and Firoozabadi, A. 2018. Methane Adsorption and Self-Diffusion in Shale Kerogen and Slit Nanopores by
- 29 Molecular Simulations. Journal of physical chemistry 122(41): 23528-23542. https://doi.org/10.1021/acs.jpcc.8b07123
- 30 Toyar, F. D., Eide, O., Graue, A. et al. 2014. Experimental Investigation of Enhanced Recovery in Unconventional Liquid 31 Reservoirs using CO₂: A Look Ahead to the Future of Unconventional EOR. Presented at the SPE Unconventional Resources
- 32 Conference, Woodlands, Texas, 1-3 April. SPE-169022-MS. https://doi.org/10.2118/169022-MS.
- 33 Vazquez, M. and Beggs, H. D. 1980. Correlations for Fluid Physical Property Prediction. Journal of Petroleum Technology
- 32(6): 968-970. https://doi.org/10.2118/6719-PA. 34
- 35 Wang, S., Feng, Q. H., Javadpour, F. et al. 2015. Oil Adsorption in Shale Nanopores and Its Effect on Recoverable Oil-in-
- 36 Place. International Journal of Coal Geology 147-148: 9-24. https://doi.org/10.1016/j.coal.2015.06.002.
- 37 Whitworth, T. M. 1993. Hyperfiltration-Induced Isotopic Fractionation: Mechanisms and Role in the Subsurface. Ph.D. Thesis,
- 38 Purdue University, West Lafayette, Indiana (January 1993).
- 39 M. R. J. 1948. Some Electrochemical **Properties** of Shales. Science **108**(2816): 684-685.
- 40 https://dx.doi.org/10.1126/science.108.2816.684.
- 41 Young, A. and Low, P. F. 1965. Osmosis in Argillaceous Rocks. American Association of Petroleum Geologists Bulletin 49(7):
- 42
- 43 Zhu, Z., Fang, C., Qiao, R. et al. 2019. Experimental and Molecular Insights on Sieving of Hydrocarbon Mixtures in Niobrara
- 44 Shale. Presented at the Unconventional Resources Technology Conference, Denver, Colorado, 22-24 July.